Field Test Results for Low Power Bearing Estimator Sensor Nodes

P. Julian[*∥], A. G. Andreou[†], G. Cauwenberghs[†], M. Stanacevic[†], H. Goldberg[‡],
P. S. Mandolesi[*¶], L. Riddle[§] and S. Shamma[**]

[*]Dep. de Ing. Eléctrica y Computadoras, Universidad Nacional del Sur, Bahía Blanca, 8000, Argentina.
[∥]Consejo Nacional de Investigaciones Científicas y Técnicas, Cap. Fed. 1033, Argentina.
[†]Dep. of Electrical and Computer Eng., Johns Hopkins University, Baltimore, MD 21218, USA.
[‡]Cornell University, New York, NY 10021 USA.
[¶]CIC Comisin de INvestigaciones Cientficas de la Provincia de Buenos Aires, Argentina
[§]Signal Systems Corporation, Baltimore-Annapolis Blvd, Suite 210 Severna Park, MD 21146 USA.
[**]Dept. of Electrical Engineering, University of Maryland, College Park, MD 20742, USA.
E-Mail:pjulian@ieee.org

Abstract— This paper describes experimental results of low power sensor nodes designed to perform bearing estimation. The nodes are intended to form a wireless sensor network able to locate an audio source. Two different nodes are tested: one is based on a Cross-correlation Derivative integrated circuit (IC), and the other on a Gradient Flow IC. Implementation details and experimental results of both systems working in a natural environment are presented.

I. INTRODUCTION

This paper describes experimental results of low power sensor nodes that perform bearing estimation. The nodes are designed to form a wireless sensor network able to locate an audio source; therefore, they must satisfy several requirements. First of all, they must be as small as possible so that they can be deployed in large quantities without being noticed, and without interfering noticeably with the environment. Second, they must have a long service time, which translates in very low power consumption (usually, in the order of microwatts). Finally, they must meet accuracy specifications to succesfully localize acoustic targets. The requirements found in networks of these characteristics often contradict each other; for instance, it is well known that the greater the distance between microphones the better a bearing estimator can measure the source sound angle. However, this opposes the minimum dimensions requirement. In all cases, there is a limitation to the achievable performance, which is a function of several factors: the separation distance between microphones, the signal–to–noise ratio of the signal, the bandwidth of the signal and the time used to perform the estimation. This limitation is quantified by the Cramér–Rao lower bound, which gives a lower bound for the variance of the estimation [1].

The application that originates the results shown in the paper is the development of a sensor node using an acoustic enclosure (ASU) with four MEMS microphones (see Fig. 1). The enclosure diameter is 11cm and its height is 2.5cm. The space for the electronics (including batteries) is located underneath the microphones enclosure and occupies a similar volume.
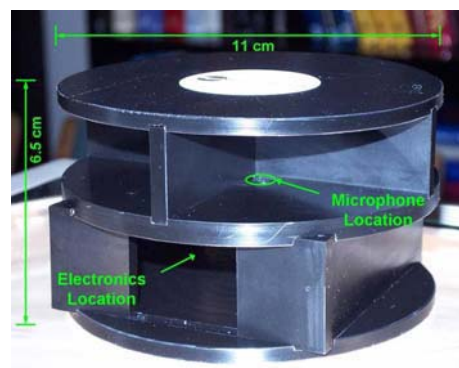

Fig. 1.   Acoustic enclosure (ASU) with microphones and electronics.

Two integrated circuits were especifically designed for the task; one of them implements a cross-correlation derivative algorithm [2] and the other a Gradient Flow algorithm [3], [4]. The design was based on signals recorded outdoors during a field test; details of the initial experiment, the algorithms and preliminary results, including a comparison with two other methods, were reported in [1].

The cross-correlation derivative (CCD) approach is a variation of the standard time-domain cross-correlation between two signals ([5], [6], [7]). It has been shown that some animals, like the barn owl utilize algorithms of this type to obtain azimuth information [8]; an analog VLSI implementation of the barn owl localization system was reported in [9]. One of the features of the CCD algorithm is that it works with a one-bit discretization of the input signals, therefore, reducing drastically the complexity of the resulting digital circuitry. Another feature is that the spatial derivative of the cross-correlation is calculated instead of the cross-correlation itself. Calculation of the CCD results in an activity reduction of a thousand times in the digital circuitry. Therefore, power consumption is reduced in a proportional factor. The reduction of activity also results in smaller values for the internal counters, thus reducing

complexity and layout space. In the case of the standard cross-correlation approach, once the partial correlations are calculated, the maximum needs to be evaluated which requires a dedicated (either analog or digital) stage. In the CCD, it is only necessary to locate a change in the output value of the partial correlations (which are either 1 or 0), making this task trivial.

In the gradient flow (GDF) approach [3], the signals recorded by the microphones are thought of as samples of a field sound wave. A linearization of the field permits to calculate the direction of the arriving sound. In this case, the calculation of the bearing angle relies on the analog value of the signal, and on the quality of the derivative of the signal. The IC described in [3] implements the algorithm using a switched-capacitor architecture at a frequency of 2KHz.

Another implementation on IC is the architecture proposed in [10] based on an analog cochlea model.

The paper is organized as follows: Section II presents a detailed description of the hardware components used in the field test; Section III shows the experimental results obtained in a natural environment; Section IV presents some conclusions.

II. HARDWARE SETUP

The starting point of the hardware setup is the microphone. Four miniature Knowless Sysonic MEMS microphones were used. These microphones exhibit a sensitivity of -42db and a noise level of 35dbA SPL. An amplification stage was designed in order to amplify the milivolt level input signal into a volt level signal. In the case of the cross-correlator, another stage with a comparator was used to clip the signal and produce a digital output. Amplifiers and comparators were implemented using commercial off-the-shelf (COTS) components.

The amplifier was designed to provide an overall amplification of 1000. The cross-correlator estimator depends directly on the phase difference of the incoming signals, therefore it is critical to minimize the mismatch between the channels. The main sources of mismatch are resistor, capacitor and finite-gain opamp channel mismatch. The first two factors are somewhat obvious; the latter is not unless we specify low-power consumption opamps. In this case, the Gain-Bandwith Product (GBP) will be small (it is proportional to power consumption), and the projected closed loop gain migh deviate from the ideal closed loop gain (CLG), particularly at higher frequencies where the open loop gain (OLG) drop is bigger.

Considering these factors, and selecting opamps with bias currents in the tens of microamps range, the design was based on the two stage amplifier configuration shown in Fig. 2. Every stage provides a gain of $A_i = 32.93$ for an input-output gain of $A_v = 1084$. The values of the components are: $R_1 = R_3 = 15K$ (1%); $R_2 = R_4 = 494K$ (1%); $C_1 = 1\mu F$ (2%), $C_2 = 680pF$ (2%), $C_3 = 100\mu F$.

Capacitor C_1 is metallized polypropelene, C_2 is film chip and C_3 is a regular electrolitic capacitor. The low cutoff frequency is set by C_1 and R_2 and is $f_L = 10.6Hz$; the high cutoff frequency is set by C_2 and R_2 and is $f_H = 473Hz$.

	A_v	f_L	f_H
Min	1127	9.60	517.5
Max	1142	9.93	534.0
Mean	1136	9.77	526.0
Sigma	7.05	7.11e-2	3.47

	10Hz	50Hz	100Hz	500Hz
Min	43.6	56.1	5.82	44.0
Max	44.8	61.0	5.39	43.1
Mean	44.3	59.0	5.62	43.6
Sigma	0.2	9.2e-2	8.9e-2	0.18

The selected opamp is a TLV2382 that features a power consumption of $7\mu A$ per channel and a GBP of 160000.

Table I summarizes maximum, minimun, mean value and σ for the closed loop gain, low cutoff and high cutoff frequencies, assuming a Gaussian distribution of the components and the opamp gain. Table II summarizes the phase mismatch at $10Hz$, $50Hz$, $100Hz$ and $500Hz$ These results are based on a Monte Carlo simulation with 100 runs.

Note from these results that phase error is below 1 degree for the range of interest. Current consumption for the four channels board is $40\mu A$; the CCD chip has a current consumption of $200\mu A$ and the GDF chip has a current consumption of $10\mu A$. All components are able to work with either $3V$ or $5V$ power supply.

III. EXPERIMENTS AND RESULTS

A field test was performed outdoors in Aberdeen Proving Ground, Aberdeen, MD, USA.

The setup under consideration is as follows: The acoustic enclosure (ASU) has four microphones; they are located pairwise $6cm$ apart, but the enclosure produces an effective separation of $L_s = 15.87cm$. It is assumed that the sound source is far away from the microphones and is also limited in frequency to the band $[10Hz, 300Hz]$. For the experiment,
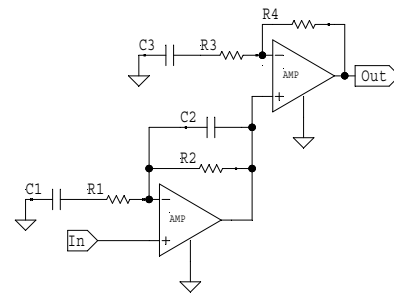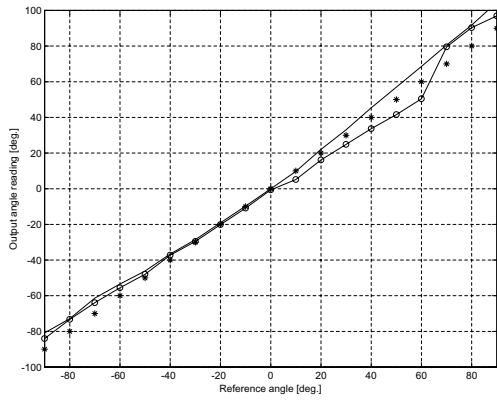

Fig. 2. Two stage amplifier.

Fig. 3. BBN: Mean value of the output in the range $[-90, +90]$. Cross-correlation results shown with circles; GDF results shown with solid line; linear output shown with asterisks.
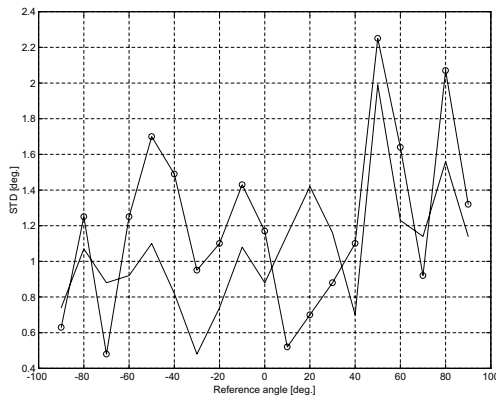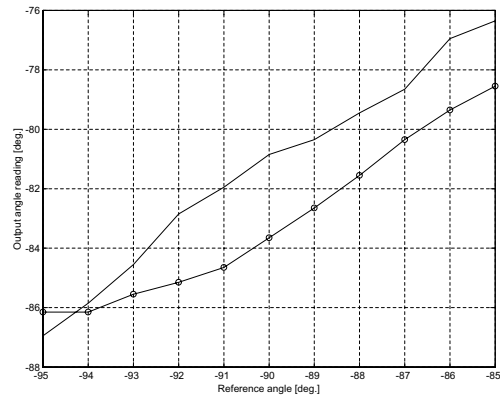

Fig. 5. BBN: Mean value of the output in the range $[-95, -85]$. Cross-correlation results shown with circles; GDF results shown with solid line.
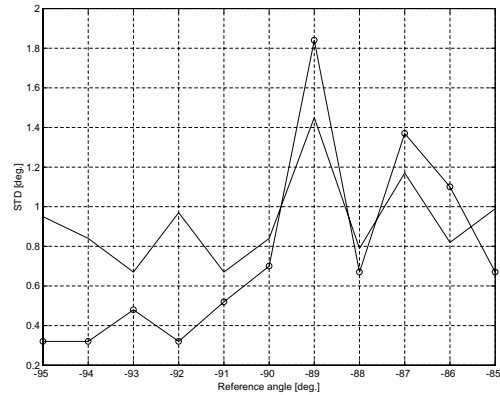

Fig. 4. BBN: STD of the output in the range $[-95, -85]$. Cross-correlation results shown with circles; GDF results shown with solid line.

Fig. 6. BBN: STD of the output in the range $[-95, -85]$. Cross-correlation results shown with circles; GDF results shown with solid line.

a speaker and an amplifier were located twenty meters away from the ASU at different angles. A signal was played through the speaker and the indication of the IC's was measured. Two different types of signals were used: broadband noise (BBN) ($[16Hz, 300Hz]$) and a narrowband signal (NBS) ($200Hz$). Three different sets of measurements were collected. In a first case (Long Range), the angle of the speaker was between -90^0 and 90^0 in steps of 10^0. In a second case (Short Range 1), the angle of the speaker was between -85^0 and -95^0 in steps of 1^0; and in a third case (Short Range 2), the angle of the speaker was between -40^0 and -50^0 in steps of 1^0. For every angle, ten different readings were obtained. Every reading was performed by the IC's in a time window of one second. The plots for the third case are not shown due to lack of space.

A. Test Using Broadband Noise

Long Range output angle mean value for both approaches is shown in Fig. 3; The standard deviation in the two cases is shown in Fig. 4. Short Range (case 1) results are shown in Figs. 5 and 6. Table III summarizes the mean STD for both algorithms in the three ranges.

B. Test Using a Narrowband Signal

Long Range output angle mean value for both approaches are shown in Fig. 7; The standard deviation in the two cases is shown in Fig. 8. Short Range (case 1) results are shown in Figs. 9 and 10. Table IV summarizes the mean STD for both algorithms in the three ranges.

IV. CONCLUSIONS

Tests results for two integrated circuits that perform bearing estimation have been presented. The objective is to develop a low-power node for an acoustic localization sensor network. Having matched channels is a key factor to achieve good resolution; a setup based on COTS has been used for the field tests. Future research includes the implementation of all the components on the same die.

TABLE III
ACCURACY OF THE ALGORITHMS (MEAN STD) IN DEGREES (BBN)

Range	[-90,+90]	[-95,-85]	[-50,-40]
GDF	1.06	0.92	0.98
CCD	1.20	0.75	1.38

TABLE IV
ACCURACY OF THE ALGORITHMS (MEAN STD) IN DEGREES (NB)

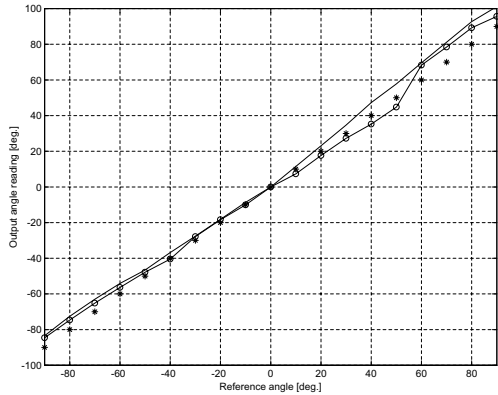| Range	[-90,+90]	[-95,-85]	[-50,-40]
GDF	1.18	0.93	1.11
CCD	0.79	0.54	1.00

Fig. 7. NBS: Mean value of the output in the range $[-90, +90]$. Cross-correlation results shown with circles; GDF results shown with solid line; linear output shown with asterisks.

Both circuits perform well with an accuracy close to one (1) degree, which was the original specification. More precision can be obtained at the expense of increasing the integrating time (1 second) and also using more precisely matched elements in the amplifying channels.

One interesting observation is that the CCD approach performs better with the narrowband signal, while the GDF approach shows better results with broadband noise. This might be due that CCD is based on interaural time differences (ITD), therefore, providing a better result in the presence of a pure tone.

REFERENCES

[1] P. Julian, A. G. Andreou, G. Cauwenberghs, L. Riddle, and A. Shamma, "A comparative study of sound localization algorithms for energy aware sensor network nodes," *IEEE Trans. Circuits Syst. I*, vol. 4, pp. 640–648, April 2004.

[2] P. Julian, A. G. Andreou, P. Mandolesi, and D. Goldberg, "A low-power CMOS integrated circuit for bearing estimation," in *Proc. of the IEEE Int. Symp. on Circuits and Syst. (ISCAS)*, vol. 5, pp. 305–308, 2003.

[3] G. Cauwenberghs, M. Stanacevic, and G. Zweig, "Blind broadband source localization and separation in miniature sensor arrays," in *Proc. of the IEEE Int. Symp. on Circuits and Syst. (ISCAS)*, vol. III, pp. 193–196, 2001.

[4] M. Stanacevic and G. Cauwenberghs, "Micropower mixed-signal acoustic localizer," in *Proc. IEEE Eur. Solid State Circuits Conf. (ESSCIRC 2003)*, (Estoril, Portugal), 2003.

[5] C. H. Knapp and G. C. Carter, "The generalized correlation method for estimation of time delay," *IEEE Trans. Acoustics, Speech, Signal Processing*, vol. ASSP-24, pp. 320–327, August 1976.

[6] G. C. Carter, "Time delay estimation for passive sonar signal processing," *IEEE Trans. Acoustics, Speech, Signal Processing*, vol. ASSP-29, pp. 463–470, June 1981.

[7] A. H. Quazi, "An overview on the time delay estimate in active and passive systems for target localization," *IEEE Trans. Acoustics, Speech, Signal Processing*, vol. ASSP-29, pp. 527–533, June 1981.

[8] A. Moiseff and M. Konishi, "Neuronal and behavioral sensitivity to binaural time differences in the owl," *J. Neuroscience*, vol. 1, pp. 40–48, 1981.

[9] J. P. Lazzaro and C. Mead, "Silicon models of auditory localization," *Neural Computation*, vol. 1, pp. 41–70, 1989.

[10] A. van Schaik and S. Shamma, "A neuromorphic sound localizer for a smart MEMS system," in *Proc. of the IEEE Int. Symp. on Circuits and Syst. (ISCAS)*, vol. IV, pp. 864–867, 2003.
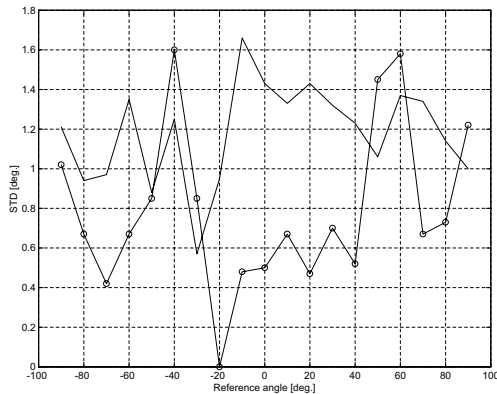
Fig. 8. NBS: STD of the output in the range $[-95, -85]$. Cross-correlation results shown with circles; GDF results shown with solid line.
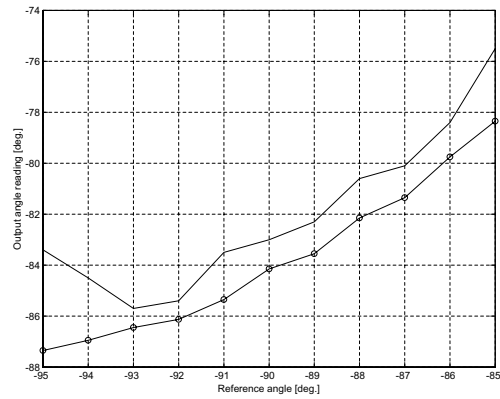

Fig. 9. NBS: Mean value of the output in the range $[-95, -85]$. Cross-correlation results shown with circles; GDF results shown with solid line.
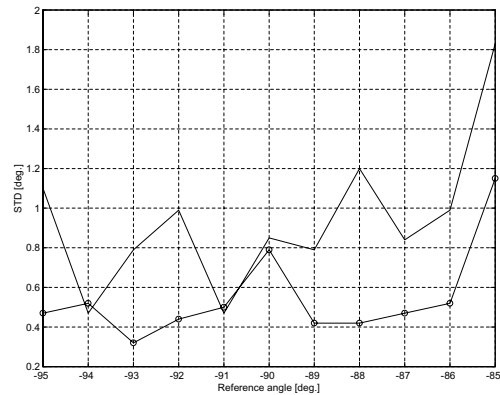

Fig. 10. NBS: STD of the output in the range $[-95, -85]$. Cross-correlation results shown with circles; GDF results shown with solid line.